

Received January 6, 2019, accepted January 23, 2019, date of publication January 31, 2019, date of current version March 7, 2019.

Digital Object Identifier 10.1109/ACCESS.2019.2896304

A Robust Watermarking Scheme in YCbCr Color Space Based on Channel Coding

YUN TAN¹, JIAOHUA QIN¹, XUYU XIANG¹, WENTAO MA¹,
WENYAN PAN¹, AND NEAL N. XIONG²

¹College of Computer Science and Information Technology, Central South University of Forestry and Technology, Changsha 410004, China

²Department of Mathematics and Computer Science, Northeastern State University, Tahlequah, OK 74464, USA

Corresponding authors: Jiaohua Qin (qinjiaohua@163.com) and Xuyu Xiang (xyuxiang@163.com)

This work was supported in part by the National Natural Science Foundation of China under Grant 61772561 and Grant 31870532, in part by the Key Research & Development Plan of Hunan Province under Grant 2018NK2012, in part by the Postgraduate Research and Innovation Project of Hunan Province under Grant CX2018B447, and in part by the Postgraduate Science and Technology Innovation Foundation of Central South University of Forestry and Technology under Grant 20183027 and Grant 20183034.

ABSTRACT The rapid development of big data and cloud computing technologies greatly accelerate the spreading and utilization of images and videos. The copyright protection for images and videos is becoming increasingly serious. In this paper, we proposed the robust non-blind watermarking schemes in YCbCr color space based on channel coding. The source watermark image is encoded and singular value decomposed. Subsequently, the singular value matrixes are embedded into the Y, Cb, and Cr components of the host image after four-level discrete wavelet transform (DWT). The embedding factor for each component is calculated based on the just-noticeable distortion and the singular vectors of HL subband of DWT. The peak signal-to-noise ratio of the watermarked image and the normalized correlation coefficient of the extracted watermark are investigated. It is shown that the proposed channel coding-based schemes can achieve near exact watermark recovery against all kinds of attacks. Considering both robustness and transparency, the convolutional code-based additive embedding scheme is optimal, which can also achieve good performance for video watermarking after extension.

INDEX TERMS Watermarking, YCbCr color space, singular value decomposition, channel coding, repetition code, convolutional code.

I. INTRODUCTION

Vision is an important means of human cognition, and more than 80% of information that human received comes from vision. It can be seen that multimedia has become the most important kind of visual information other than text. At the same time, the rapid development of big data and cloud computing technologies has greatly accelerated the spreading and utilization of images and videos. Therefore, copyright protection for images and videos is becoming increasingly serious.

Watermarking is used widely for copyright protection, which embeds information imperceptibly in the host data with hidden algorithms and keys. It can help to identify the source and destination of images and videos. The requirements for watermarking mainly include two sides [1].

The associate editor coordinating the review of this manuscript and approving it for publication was Zhaoqing Pan.

A. IMPERCEPTIBILITY

The embedded watermark is expected to have perceptual transparency and imperceptibility. And it will not introduce perceptible artifacts to the original images or videos.

B. ROBUSTNESS

The watermark should be robust enough against data distortions introduced by data processing or system noise. In the complicated big data environment, the watermarks also need to resist the threat of various attacks, such as the damage, destruction or removal of embedded watermarks.

In order to meet the above two requirements of watermarking, many researchers have conducted deep research and achieved many improvements. But most of the results are for grayscale images. The watermarking algorithms for color images and videos are still comparatively less.

For color images and videos, the color model is a basic abstract mathematical method that describes color represent

using a set of color components. There are several different color spaces can be chosen for watermarking, such as RGB, YCbCr, CMYK, YUV, Lab, etc. In [2], watermarking techniques in the color channels of RGB, YUV, YCbCr color spaces were studied and comparative performances were analyzed. It was proved that the watermarking embedding in YCbCr color space was more robust and transparent compared to that in RGB and YUV color space. Therefore, we choose YCbCr color space in our research.

The earlier scheme based on YCbCr color space was proposed by Hsieh *et al.* [3], which used just-noticeable-distortion (JND) model and wavelet transform to insert watermarking. Some researchers used Singular Values Decomposition (SVD) [4] and Discrete Cosine Transform (DCT) [5] to enhance the robustness of watermark. Arnold chaotic based schemes [6], [7] were also proposed to reduce the false detection. At the same time, the human visual system (HVS) in color images was considered [8] and the three channels of YCbCr color space were usually partially used [9], [10] in order to achieve better invisibility. Recently, Roy *et al.* [11] proposed an HVS inspired robust watermarking scheme, which used the Cb component to embed SV information of the watermark. The additive and multiplicative embedding schemes (AES/MES) were analyzed and demonstrated. It was proved that the AES scheme could provide better perceptual quality and robustness against attacks compared to existing schemes, but it was sensitive to singular vector (SV) attack. The MES scheme was proposed to increase the robustness against SV attack, but the PSNR and robustness against other attacks (noise, rotation, cropping, etc.) were decreased.

From the above, it can be seen that in traditional schemes there is usually a tradeoff between imperceptibility and robustness in the design of the watermarking scheme. On the one hand, the impact of the watermark to the host image should be minimized to meet the requirement of imperceptibility. On the other hand, the embedded watermark should keep the amplitude as high as possible to ensure the robustness.

In latest improvements, some schemes considered to increase the redundancy of embedded information or separate the secret information into several parts during insertion, such as arithmetic coding scheme [12], combined-decision-based scheme [13], DADBS (Dual Adjusted Direct Binary Search) scheme [14], etc. It was shown that the redundancy and separation of secret information could achieve some improvement of robustness and transparency. Therefore, we consider introducing channel coding into the watermarking scheme in this work.

Channel coding theory was proposed by Shannon in 1948 [15]. It is shown that error determination and error correction can be achieved at the receiver with the insertion of some symbols into the source data stream, which greatly increases the reliability of communication and enhances the ability of anti-interference [16]. Therefore, channel coding has been applied widely in communication systems. It was

also introduced in watermarking schemes to increase the robustness [17]–[22]. Turbo codes based on the DCT coefficients were introduced in [17]. Bao *et al.* [18] proposed a method based on Slant Transform and channel coding. Watermarks were inserted in LSB of each pixel to achieve blind extraction. In [19], the original image was source coded using an appropriate channel code. Associated with parity bits and check bits, this scheme could detect the tampered area and recover the lost information. Dual watermark was designed in [20] to locate the tampering and restore the image while check bits of source channel coding were used to detect tampering. Sarreshtedari *et al.* [24] designed a self-embedding scheme for JPEG images based on modeling the tampering as a source channel coding problem. It showed better robustness and image quality compared to existing JPEG domain self-embedding schemes.

From above, it can be seen that the channel coding is a potential method for watermarking, but the channel coding based schemes are still limited. In this paper, we propose a robust watermarking scheme in YCbCr color space based on channel coding, which is an improvement of the AES/MES scheme proposed by Roy [11]. Firstly, the source watermark image is encoded and singular value decomposed. The singular value matrixes are embedded into the Y, Cb and Cr components of the host image after four-level DWT. The embedding factor for each component is calculated based on the JND and the singular vectors of HL subband of DWT. This scheme is also extended for video watermarking by inserting the singular value matrixes of encoded bits separately into the selected keyframe group.

The paper is organized as follows: the preliminary of YCbCr color space and channel coding is given in Sec.2 and Sec.3. Then, the proposed schemes are introduced in Sec.4. Simulations results and comparisons between the proposed schemes and existing schemes are shown in Sec.5. Finally, we conclude this paper in Sec.6.

II. YCbCr COLOR SPACE

YCbCr is a kind of linear color space, in which Y denotes the luminance component while Cb and Cr are the concentration offset components of blue and red. RGB can be converted to YCbCr by following equations [2]:

$$\begin{aligned} Y &= 0.299R + 0.587G + 0.114B \\ Cb &= 0.596R - 0.272G - 0.321B \\ Cr &= 0.212R - 0.523G - 0.311B \end{aligned} \quad (1)$$

Reversibly, YCbCr to RGB conversion is as follows:

$$\begin{aligned} R &= Y + 0.956Cb + 0.620Cr \\ G &= Y - 0.272Cb - 0.647Cr \\ B &= Y - 1.108Cb + 1.705Cr \end{aligned} \quad (2)$$

Assuming the color variables of YCbCr channels in the host image as U_Y , U_{Cb} and U_{Cr} , the color variables become U'_Y , U'_{Cb} and U'_{Cr} with watermark insertion. Therefore, the overall changes of the host image I brought by

watermark embedding can be expressed as [11]

$$\begin{aligned} \Delta I = & \frac{\partial I}{\partial U_Y} \Delta U_Y + \frac{\partial I}{\partial U_{Cb}} \Delta U_{Cb} + \frac{\partial I}{\partial U_{Cr}} \Delta U_{Cr} \\ & + R_{YCb} \cdot \frac{\partial^2 I}{\partial U_Y \partial U_{Cb}} (\Delta U_Y \cdot \Delta U_{Cb}) \\ & + R_{YCr} \cdot \frac{\partial^2 I}{\partial U_Y \partial U_{Cr}} (\Delta U_Y \cdot \Delta U_{Cr}) \\ & + R_{CbCr} \cdot \frac{\partial^2 I}{\partial U_{Cb} \partial U_{Cr}} (\Delta U_{Cb} \cdot \Delta U_{Cr}) \end{aligned} \quad (3)$$

where

$$\begin{aligned} \Delta U_Y &= U'_Y - U_Y \\ \Delta U_{Cb} &= U'_{Cb} - U_{Cb} \\ \Delta U_{Cr} &= U'_{Cr} - U_{Cr} \end{aligned} \quad (4)$$

and

$$\begin{aligned} R_{YCb} &= \frac{E[\Delta U_Y \cdot \Delta U_{Cb}]}{\sigma_Y \sigma_{Cb}} \approx \frac{\Delta U_Y \cdot \Delta U_{Cb}}{\sigma_Y \sigma_{Cb}} \\ R_{YCr} &= \frac{E[\Delta U_Y \cdot \Delta U_{Cr}]}{\sigma_Y \sigma_{Cr}} \approx \frac{\Delta U_Y \cdot \Delta U_{Cr}}{\sigma_Y \sigma_{Cr}} \\ R_{CbCr} &= \frac{E[\Delta U_{Cb} \cdot \Delta U_{Cr}]}{\sigma_{Cb} \sigma_{Cr}} \approx \frac{\Delta U_{Cb} \cdot \Delta U_{Cr}}{\sigma_{Cb} \sigma_{Cr}} \end{aligned} \quad (5)$$

σ_Y , σ_{Cb} and σ_{Cr} are the standard deviations of the YCbCr channel color variables. The imperceptibility of watermark requires that the image modification introduced by watermark insertion should be as small as possible. This means that we should try to minimize ΔI during the design of the watermarking scheme. In YCbCr color spaces, the correlation coefficients R_{YCb} , R_{YCr} and R_{CbCr} are smaller since the color channels are more independent compared to other color spaces such as RGB [20]. Therefore, we choose YCbCr color space in our watermarking scheme.

Considering the energy occupation of the three channels of YCbCr color space, there is most energy in the Y channel [11]. While considering the color sensitivity of HVS, the Cb channel is least sensitive [22]. This means that the scheme of embedding watermark information in Y channel is more robust, while watermark insertion in the Cb channel has better performance of transparency. In previous research, usually only one channel is chosen with the tradeoff between robustness and imperceptibility. In this paper, we try to make use of the two or all three channels for watermark embedding to combine the advantages of each channel.

III. CHANNEL CODING

Channel coding theorem [15]: Assume that the channel capacity is C , then for any coding rate $R < C$, there is a type of channel code that can achieve arbitrarily low decoding error rate when the code length increases, as

$$p \leq Ae^{-nE(R)} \quad (6)$$

where p is the decoding error bit, n is the code length and $E(R)$ is the positive real number function of R .

A. REPETITION CODE

Repetition code is a kind of block code. Assume that the original bit stream is $[b_1 b_2 \dots b_n]$, then the $(k, 1)$ repetition encoded bit stream is $(b_1 \dots b_1 b_2 \dots b_2 \dots b_n \dots b_n)$, where every bit is repeated for k times. At the receiver side, decoding is implemented based on the bits number of 0 and 1 if k is an odd number. If the number of "0" is $n_0 > k/2$, then the received codeword will be decoded as "0", else it will be decoded as "1". While if k is even, it is possible that the numbers of "0" and "1" are equal as $n_0 = n_1 = k/2$. Therefore it is infeasible to decode only based on the bits number of "0" and "1". This kind of incomplete decoding needs the association of other methods such as automatic repeat request mechanism [23].

The decoding bit error rate will decrease with the increment of coding length k . Assuming the transmission error probability as P_e , the error decoding probability is

$$\begin{aligned} p = 1 - & [(1 - p_e)^k + \binom{k}{1} p_e (1 - p_e)^{k-1} + \dots \\ & + \binom{k}{[k/2]} p_e^{[k/2]} (1 - p_e)^{k-[k/2]}] \end{aligned} \quad (7)$$

In this work, we use a modified repetition code with repetition length as 2. Assuming the source bit stream as $(b_1 b_2 \dots b_n)$, then the encoded bit stream is $(b_1, 1-b_1, b_2, 1-b_2, \dots, b_n, 1-b_n)$. Assuming the received code stream as $(c_1, c_2, \dots, c_{2n})$, then we can decode the bit stream $(b'_1 b'_2 \dots b'_n)$ with

$$b'_i = \begin{cases} 1, & \text{if } c_{2i-1} - c_{2i} > 0 \\ 0, & \text{if } c_{2i-1} - c_{2i} \leq 0, \end{cases} \quad 1 \leq b \leq n \quad (8)$$

Then the error decoding probability is

$$p = 1 - [(1 - p_e)^2 + 2p_e(1 - p_e)] = p_e^2 \quad (9)$$

It can be seen that the error decoding probability is decreased to the square of propagation error probability with the (2,1) repetition code.

B. CONVOLUTIONAL CODE

For the general block codes, usually the check codes are only related to the bits of the same group and independent of the bits of the other groups. Convolutional code was proposed by Elias in 1955. Its check codes are not only related to the bits of the same group, but also related to the bits of the previous encoded groups. Since convolutional code makes full use of the correlation between the bit groups during the coding process, it is proved to have better performance than general block codes.

Convolutional code is often expressed as (n, k, N) , which means every input k bits will be encoded to n output bits. N is the encoding constraint length, which indicates the number of code blocks that are mutually constrained in the encoding process. The coding rate R is define as

$$R = \frac{k}{n} \quad (10)$$

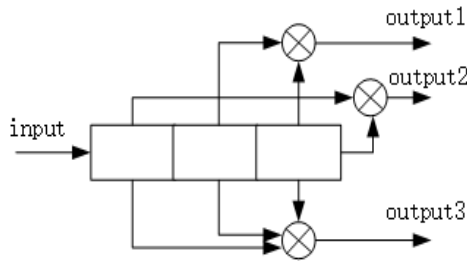


FIGURE 1. Convolutional encoder of (3, 1, 3).

The bit error rate (BER) of the system will decrease with the increment of N and the reduction of R . However, the complexity of encoding and decoding will increase. In order to obtain the best compromise between bit error rate and complexity, we choose a typical (3, 1, 3) convolutional encoder in this work. The structure is shown in Figure 1.

For the decoding of convolutional code, we use the Viterbi decoding algorithm. It is a maximum likelihood decoding algorithm based on the trellis graph, which is also an optimal probability decoding algorithm. The error decoding probability of Viterbi decoding is given by [24]

$$p \approx A_{d_f} 2^{d_f} P_e^{d_f/2} \quad (11)$$

where A_{d_f} is the number of code sequences with weight d in the convolutional codes, d_f is the free distance of the codes and P_e is the transmission error probability. The decoding error will decrease with the lower coding rate and bigger minimum distance of the codes.

IV. PROPOSED WATERMARKING SCHEME

The additive embedding scheme (AES) proposed by Roy *et al.* [11] has overcome all the previous schemes on the performance against most attacks except singular value (SV) attack. In order to increase the robustness against SV attack, the multiplicative embedding scheme (MES) was proposed. This scheme showed better performance for SV attack, but the PSNR was decreased and the performance for other attacks (noise, rotation, cropping, etc.) was not as good as AES. At the same time, the AES/MES algorithms used the Cb component to embed watermark, therefore the PSNR was closely related to the Cb component. Because of the different energy distribution of the Y, Cb and Cr components in different types of images, the PSNR of watermarked images has big variety. In order to achieve more stable robustness for all attacks and wider applicability for different images, we propose a channel coding based watermark embedding scheme in YCbCr space.

A. WATERMARK EMBEDDING ALGORITHM

Our scheme is shown as Figure 2. On the one hand, the watermark image is transformed to the binary image and scrambled by Anordl transform. Then the bits stream are channel coded and the encoded bits are split and reshaped to 3 matrixes (coding rate $R = 1/3$). SVD is performed for these matrixes. On the other hand, the original host image is converted to YCbCr color space and 4-level DWT is performed for Y, Cb and Cr components. Then the HL subband is singular vector decomposed. Finally, the S vectors of the encoded watermark are embedded in Y, Cb and Cr components and the watermarked image is generated.

Theoretically, any type of channel coding can be applied in our scheme. The minimum distance and the redundancy of the codes will have an impact on the watermark performance. The robustness will be better with higher redundancy and bigger minimum distance of the codes. With the consideration of encoding and decoding complexity, we mainly focus on the repetition coding and convolutional coding with coding rate as 1/2 and 1/3 in this paper. The watermark strength factor is calculated based on the just noticeable distortion (JND) and the singular vectors [11]. Then the singular vectors of the channel components are updated additively by the singular value of the watermark. The detailed algorithm is described in Algorithm 1.

Another embedding method of the watermark is the multiplicative scheme proposed by Roy *et al.* [11]. The strength factor of the watermark is calculated based on the mean value of JND instead of minimum value. The singular values of the channel components are updated by the multiplied singular values of the watermark. The channel coding based multiplicative embedding scheme is described in Algorithm 2.

B. WATERMARK EXTRACTION ALGORITHM

The watermark extraction process is reverse to the embedding process as figure.3. Firstly, the watermarked image is converted to YCbCr color space and 4-level DWT is performed. The singular values of the watermark are extracted from the singular values of the channel components. We calculate the encoded bits of the watermark and reshape them to bits sequence as the input of the channel decoder. The decoded bits are reshaped and Anordl transformed inversely, then the extracted watermark is achieved. For additive embedding scheme and multiplicative embedding scheme, the watermark extraction process is similar as described in Algorithm 3.

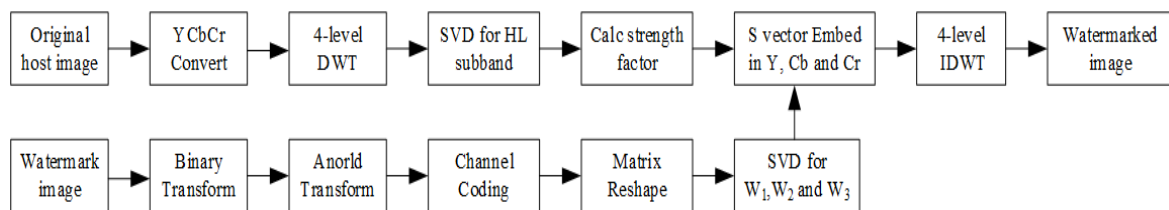


FIGURE 2. The proposed watermarking scheme based on channel coding (coding rate = 1/3).

Algorithm 1 Channel Coding Based Additive Embedding Scheme

- 1: **Input:** color host image (H), watermark image (W), Anorl transform key
- 2: **Output:** watermarked image H_w
- 3: Read host image H with the size of [1024,1024].
- 4: Convert RGB image to YCbCr color space with equation (1).
- 5: Read watermark image W with the size of [64,64] and convert it to binary image W_b .
- 6: Perform Anorl transform on the binary image W_b .
- 7: Reshape the matrix W_b to vector and input it to the channel encoder (repetition encoder or convolutional encoder). Assume that the encoded bit stream is W_c .
- 8: Split bit stream W_c to 3 sequences (assuming the coding rate as $R = 1/3$) and reshape them to three matrixes W_1 , W_2 and W_3 .
- 9: Apply SVD to W_1 , W_2 and W_3 and achieve the singular value matrixes S_{w1} , S_{w2} , S_{w3}
 $(U_{w1}, S_{w1}, V_{w1}) = \text{svd}(W_1)$
 $(U_{w2}, S_{w2}, V_{w2}) = \text{svd}(W_2)$
 $(U_{w3}, S_{w3}, V_{w3}) = \text{svd}(W_3)$
- 10: Perform 4-level two-dimensional DWT on the Y, Cb and Cr components of the host image. Subband components LL, LH, HL and HH are achieved.
- 11: Apply SVD to HL subband of the fourth DWT as
 $(U_Y, S_Y, V_Y) = \text{svd}(h14_Y)$
 $(U_{Cb}, S_{Cb}, V_{Cb}) = \text{svd}(h14_{Cb})$
 $(U_{Cr}, S_{Cr}, V_{Cr}) = \text{svd}(h14_{Cr})$
- 12: Calculate watermark strength factor k_Y , k_{Cb} , k_{Cr} for different host channels Y, Cb and Cr as

$$k_Y = \frac{|\delta_S|}{S_{w1}(1,1)} = \frac{\min \left\{ \frac{jnd(r,s,i,j)}{|U_Y \cdot V_Y^T(i,j)|} \right\}}{S_{w1}(1,1)}$$

$$k_{Cb} = \frac{|\delta_S|}{S_{w2}(1,1)} = \frac{\min \left\{ \frac{jnd(r,s,i,j)}{|U_{Cb} \cdot V_{Cb}^T(i,j)|} \right\}}{S_{w2}(1,1)}$$

$$k_{Cr} = \frac{|\delta_S|}{S_{w3}(1,1)} = \frac{\min \left\{ \frac{jnd(r,s,i,j)}{|U_{Cr} \cdot V_{Cr}^T(i,j)|} \right\}}{S_{w3}(1,1)}$$

- 13: Embed watermark information groups to host components Y, Cb and Cr as
 $S_{Y_new} = S_Y + k_Y S_{w1}$
 $S_{Cb_new} = S_{Cb} + k_{Cb} S_{w2}$
 $S_{Cr_new} = S_{Cr} + k_{Cr} S_{w3}$
- 14: Update HL subband component as
 $h14_{Y_new} = U_Y S_{Y_new} V_Y^T$
 $h14_{Cb_new} = U_{Cb} S_{Cb_new} V_{Cb}^T$
 $h14_{Cr_new} = U_{Cr} S_{Cr_new} V_{Cr}^T$
- 15: Apply four-level IDWT for host components Y, Cb and Cr.
- 16: Convert watermarked YCbCr image to RGB image H_w with equation (2).

Algorithm 2 Channel Coding Based Multiplicative Embedding Scheme

- 1: **Input:** color host image (H), watermark image (W), Anorl transform key
- 2: **Output:** watermarked image H_w
- 3: Repeat step 3-11 as in Algorithm 1.
- 4: Calculate watermark strength factor k_Y , k_{Cb} , k_{Cr} for different host channels Y, Cb and Cr as

$$k_Y = \frac{|\delta_S|}{S_{w1}(1,1)} = \frac{\text{mean} \left\{ \frac{jnd(r,s,i,j)}{|U_Y \cdot V_Y^T(i,j)|} \right\}}{S_{w1}(1,1)}$$

$$k_{Cb} = \frac{|\delta_S|}{S_{w2}(1,1)} = \frac{\text{mean} \left\{ \frac{jnd(r,s,i,j)}{|U_{Cb} \cdot V_{Cb}^T(i,j)|} \right\}}{S_{w2}(1,1)}$$

$$k_{Cr} = \frac{|\delta_S|}{S_{w3}(1,1)} = \frac{\text{mean} \left\{ \frac{jnd(r,s,i,j)}{|U_{Cr} \cdot V_{Cr}^T(i,j)|} \right\}}{S_{w3}(1,1)}$$

- 5: Embed watermark information groups to host components Y, Cb and Cr as
 $S_{Y_new} = k_Y S_Y W_1$
 $S_{Cb_new} = k_Y S_{Cb} W_2$
 $S_{Cr_new} = k_Y S_{Cr} W_3$
- 6: Apply SVD to S_{Y_new} , S_{Cb_new} and S_{Cr_new} as
 $(U_{Y1}, S_{Y1}, V_{Y1}) = \text{svd}(S_{Y_new})$
 $(U_{Cb1}, S_{Cb1}, V_{Cb1}) = \text{svd}(S_{Cb_new})$
 $(U_{Cr1}, S_{Cr1}, V_{Cr1}) = \text{svd}(S_{Cr_new})$
- 7: Update HL subband component as
 $h14_{Y_new} = U_Y S_{Y1} V_Y^T$
 $h14_{Cb_new} = U_{Cb} S_{Cb1} V_{Cb}^T$
 $h14_{Cr_new} = U_{Cr} S_{Cr1} V_{Cr}^T$
- 8: Apply four-level IDWT for host components Y, Cb and Cr.
- 9: Convert watermarked YCbCr image to RGB image H_w with equation (2).

extension of still images watermarking [25]. There are some new challenges. Firstly, there are usually many scenes in one video, which means that the texture, luminance and color features are variable for different frames. Secondly, there are more than 25 frames of images every second in video, which means that the calculation complexity is critical for video watermarking. Therefore, watermarking technology for video has also become a research hotspot recently. There are many researchers focusing on this issue. Li *et al.* [26] used the DC coefficient to embed watermark. Cedillo-Hernandez *et al.* [27] exploited the spatiotemporal properties of video and proposed a saliency-modulated JND profile for video watermarking. Shanmugam *et al.* [28] proposed a 2-level DWT-SVD based watermarking scheme for video. But the PSNR and the recovery accuracy are still not so satisfactory. We extend the proposed channel coding based watermarking scheme to video in this work.

In order to decrease the embedding and extraction complexity, we only embed the watermark in partial frames of the video, which we call keyframe groups. The keyframes are predefined and the number of keyframes is dependent on the application requirement. Firstly, we need to search for the

C. WATERMARKING SCHEME EXTENSION FOR VIDEO

A video is constructed by many frames of images. It is natural to extend the watermark embedding algorithm for video. But video watermarking is not only a simple

Algorithm 3 Watermark Extraction

- 1: **Input:** color watermarked image (H_w), watermark image (W), host image(H), Anorld transform key
- 2: **Output:** watermark image (W)
- 3: Read color watermarked image (H_w) with the size of [1024,1024].
- 4: Convert RGB image to YCbCr color space with equation (1).
- 5: Perform 4-level two-dimensional DWT on the Y, Cb and Cr components of the watermarked image. Subband components LL, LH, HL and HH are achieved.
- 6: Apply SVD to HL subband of the fourth DWT as
 $(U_Y, S_Y, V_Y) = \text{svd}(h14_Y)$
 $(U_{Cb}, S_{Cb}, V_{Cb}) = \text{svd}(h14_{Cb})$
 $(U_{Cr}, S_{Cr}, V_{Cr}) = \text{svd}(h14_{Cr})$
- 7: Extract watermark information by
 $S_{w1_new} = (S_Y - S_{Y_orig})/k_Y$
 $S_{w2_new} = (S_{Cb} - S_{Cb_orig})/k_{Cb}$
 $S_{w3_new} = (S_{Cr} - S_{Cr_orig})/k_{Cr}$
 S_{Y_orig} , S_{Cb_orig} and S_{Cr_orig} are the singular value matrixes of Y, Cb and Cr components of host image.
- 8: Calculate encoded bits matrixes as
 $Wf_1 = U_{w1} S_{w1_new} V_{w1}^T$
 $Wf_2 = U_{w2} S_{w2_new} V_{w2}^T$
 $Wf_3 = U_{w3} S_{w3_new} V_{w3}^T$
- 9: The elements of Wf_1 , Wf_2 and Wf_3 are hard judged to bits '0' or '1' according to

$$W_k(i, j) = \begin{cases} 0, & \text{if } Wf_k(i, j) \leq 0 \\ 1, & \text{if } Wf_k(i, j) > 0 \end{cases}, \quad (k = 1, 2, 3)$$
- 10: Reshape W_1 , W_2 and W_3 to vector and combine them to encoded bit stream W_c .
- 11: Input bit stream W_c to channel decoder and get the decoded bit stream W_s .
- 12: Reshape the matrix W_s to the matrix with the size of [64,64].
- 13: Apply inverse Anorld transform and achieve the extracted watermark image W_e .

other frames that are most similar to the keyframes. This is a similar problem to image retrieval. How to measure the similarity between frames is a hot topic and appropriate features need to be chosen firstly. In this paper, we assume that only one keyframe is predefined for simplicity. In previous work, it is proved that the GIST feature can represent scene information well [29], [30]. Therefore, we rank the frames based on GIST feature similarity and choose the two advanced frames as the host images. These found two frames(assumed as H_2 and H_3) and the keyframe(assumed as H_1) are defined as one group for watermarking. The encoded watermark is split into 3 parts and embedded into the three host images. The process of video watermarking is shown as figure.4. The detailed algorithm is described in Algorithm 4.

For watermark extraction in the video, the first step is to search for the host frames group. Correspondingly to

Algorithm 4 Channel Coding Based Video Watermark Embedding Scheme

- 1: **Input:** color host video (M), watermark image(W), Anorld transform key, keyframe(H_1)
- 2: **Output:** watermarked video (M_w)
- 3: Convert video to frames. Assuming the frame number as n , the frames are M_1, \dots, M_n .
- 4: Extract the GIST feature for all the frames as $G_i = \text{GIST_descriptor}(M_i)$, $i = 1 \sim n$.
- 5: Assuming the GIST vector of key frame H_1 as G_0 , calculate the Euclidean distance as the similarity measure function:
 $D_i = \|G_i - G_0\|$, $i = 1 \sim n$
 where $\|\cdot\|$ denotes the 2-norm of the computed GIST difference vector. Choose the two frames with minimum D as the host image H_2 and H_3 .
- 6: Resize the host images H_1 , H_2 and H_3 to [1024,1024].
- 7: Convert RGB images H_1 , H_2 and H_3 to YCbCr color space with equation (1) as
 $(Y_{H1}, Cu_{H1}, Cv_{H1}) = \text{RgbToYcuv}(R_{H1}, G_{H1}, B_{H1})$
 $(Y_{H2}, Cu_{H2}, Cv_{H2}) = \text{RgbToYcuv}(R_{H2}, G_{H2}, B_{H2})$
 $(Y_{H3}, Cu_{H3}, Cv_{H3}) = \text{RgbToYcuv}(R_{H3}, G_{H3}, B_{H3})$
- 8: Repeat step 5-9 as in Algorithm 1.
- 9: Perform 4-level two-dimensional DWT on the Cb component of the host images. Subband components LL,LH,HL and HH are achieved.
- 10: Apply SVD to HL subband of the fourth DWT for the three host images as
 $(U_1, S_1, V_1) = \text{svd}(h14_{H1})$
 $(U_2, S_2, V_2) = \text{svd}(h14_{H2})$
 $(U_3, S_3, V_3) = \text{svd}(h14_{H3})$
- 11: Calculate watermark strength factor k_1 , k_2 , k_3 for the different host images as

$$k_1 = \frac{|\delta_{S1}|}{S_{w1}(1,1)} = \frac{\min \left\{ \frac{jnd(r,s,i,j)}{|U_1 \cdot V_1^T(i,j)|} \right\}}{S_{w1}(1,1)}$$

$$k_2 = \frac{|\delta_{S2}|}{S_{w2}(1,1)} = \frac{\min \left\{ \frac{jnd(r,s,i,j)}{|U_2 \cdot V_2^T(i,j)|} \right\}}{S_{w2}(1,1)}$$

$$k_3 = \frac{|\delta_{S3}|}{S_{w3}(1,1)} = \frac{\min \left\{ \frac{jnd(r,s,i,j)}{|U_3 \cdot V_3^T(i,j)|} \right\}}{S_{w3}(1,1)}$$
- 12: Embed watermark information groups into the Cb component of the host images by
 $S_{1_new} = S_1 + k_1 S_{w1}$
 $S_{2_new} = S_2 + k_2 S_{w2}$
 $S_{3_new} = S_3 + k_3 S_{w3}$
- 13: Update HL subband components as
 $h14_{H1_new} = U_1 S_{1_new} V_1^T$
 $h14_{H2_new} = U_2 S_{2_new} V_2^T$
 $h14_{H3_new} = U_3 S_{3_new} V_3^T$
- 14: Apply four-level IDWT for the Cb component of the host images.
- 15: Convert watermarked YCbCr images to RGB images H_{w1} , H_{w2} , H_{w3} with equation (2).
- 16: Convert frames to video. The watermarked video (M_w) is generated.

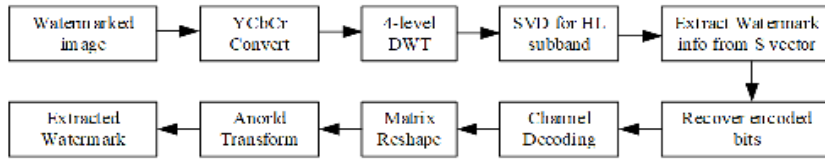


FIGURE 3. The proposed watermark extraction process.

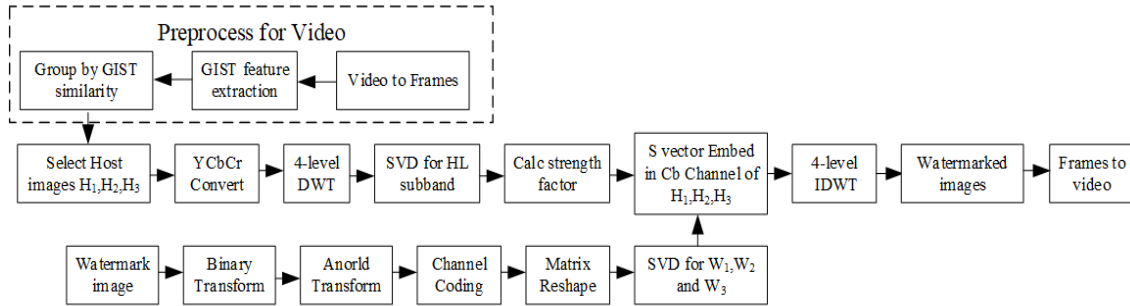


FIGURE 4. Proposed video watermark embedding scheme based on channel coding.

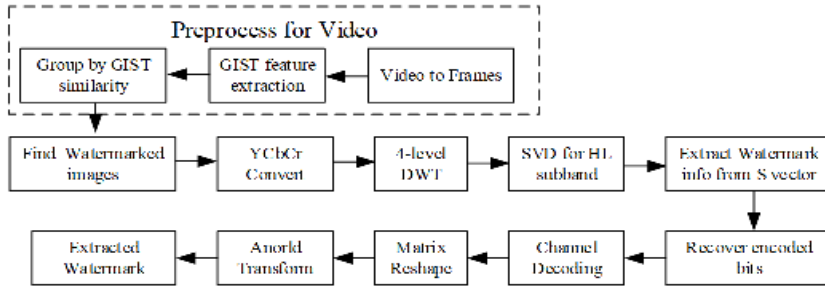


FIGURE 5. Proposed video watermark extraction.

Algorithm 5 Watermark Extraction for Video

- 1: **Input:** watermarked video (M_w), Anorid transform key, keyframe(H_1)
- 2: **Output:** watermark image (W)
- 3: Repeat step 3-7 as in Algorithm 4.
- 4: Perform 4-level two-dimensional DWT on the Cb component of the host images. Subband components LL, LH, HL and HH are achieved.
- 5: Apply SVD to HL subband of the fourth DWT for the three host images as
 $(U_1, S_1, V_1) = \text{svd}(h14_img1)$
 $(U_2, S_2, V_2) = \text{svd}(h14_img2)$
 $(U_3, S_3, V_3) = \text{svd}(h14_img3)$
- 6: Extract watermark information by
 $S_{w1_new} = (S_1 - S_{1_orig})/k_1$
 $S_{w2_new} = (S_2 - S_{2_orig})/k_2$
 $S_{w3_new} = (S_3 - S_{3_orig})/k_3$
 S_{1_orig} , S_{2_orig} and S_{3_orig} are the singular value matrixes of the Cb component of the host images.
- 7: Repeat step 8-13 in Algorithm 3.

embedding, we still use the GIST feature to measure the similarity. The two frames that have the most similar GIST vector to the keyframe are recognized as the host images

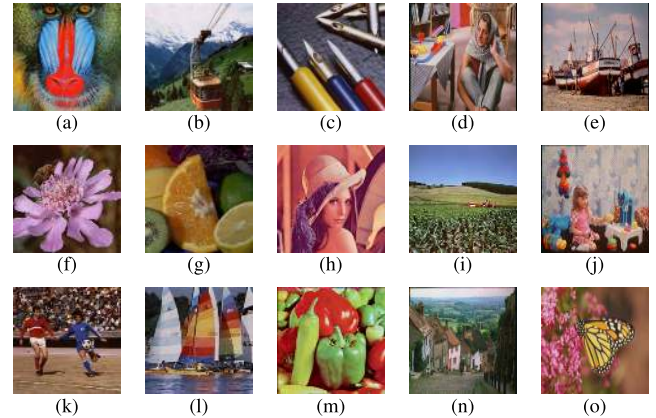


FIGURE 6. Test images. (a) Baboon. (b) Cable car. (c) Pens. (d) Barbara. (e) Boats. (f) Flower. (g) Fruits. (h) Lenna. (i) Cornfield. (j) Girl. (k) Soccer. (l) Yacht. (m) Pepper. (n) Gold hill. (o) Monarch.

H_2 and H_3 . The process of watermark extraction is an inverse process of embedding as figure.5.

The algorithm is described in Algorithm 5.

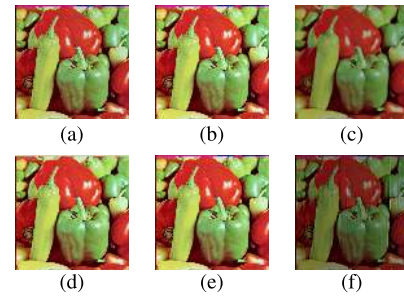
V. SIMULATIONS AND RESULTS ANALYSIS

A. SIMULATIONS FOR IMAGES

The AES proposed by Roy *et al.* [11] has overcome the previous schemes on the performance against most attacks (noise,

TABLE 1. PSNR comparison.

Image		PSNR(dB)				
Name	Size(Pixels)	AES	MES	RCAES	CCAES	CCMES
Baboon	500 × 480	38.7146	32.4812	31.3753	31.3719	25.5074
Cable car	512 × 480	52.0737	47.2594	44.1894	44.1881	34.2326
Pens	512 × 480	54.9161	48.7302	47.6100	47.5415	32.4518
Barbara	720 × 576	52.3509	45.6920	37.0853	37.0854	33.0511
Boats	787 × 576	55.9487	47.5397	43.6860	43.6839	33.8300
Flower	512 × 480	55.7980	50.0316	49.1020	49.0960	35.1883
Fruits	512 × 480	56.5215	49.6703	46.6250	46.6221	37.3354
Lenna	512 × 512	47.6097	43.3345	41.3987	41.3984	31.9475
Cornfield	512 × 480	53.7405	48.3134	42.4464	42.4476	31.7760
Girl	720 × 576	52.0935	42.7808	44.5341	44.4992	35.8343
Soccer	512 × 480	54.2910	46.4539	45.5651	45.5669	31.9731
Yacht	512 × 480	54.4099	47.0960	45.0412	45.0354	33.2960
Pepper	512 × 512	44.0641	31.2790	39.1808	39.1678	24.9802
Gold hill	720 × 576	50.0861	46.3387	41.3382	41.3379	33.9387
Monarch	768 × 512	60.1045	40.0976	43.4691	43.4606	27.6963

**FIGURE 7.** Cover images Pepper with different methods. (a) Original. (b) Watermarking with AES (PSNR = 44.0641dB). (c) Watermarking with MES (PSNR = 31.2790dB). (d) Watermarking with RCAES (PSNR = 39.1808dB). (e) Watermarking with CCAES (PSNR = 39.1678dB). (f) Watermarking with CCMES (PSNR = 24.9802dB).

rotation, cropping, etc.) except for SV attack. The MES shows better performance for SV attack, but the performance for other attacks is not as good as AES. Therefore, we compare the performance of the proposed channel coding based schemes with the AES and MES algorithm for all the attacks. We use Matlab R2013b to simulate the algorithms. The proposed repetition coding based additive embedding scheme (RCAES), convolutional coding based additive embedding scheme (CCAES) and convolutional coding based multiplicative embedding scheme (CCMES)

are investigated. The coding rate of repetition code is set as 1/2 and the coding rate of convolutional code is set as 1/3. Fifteen types of standard test images are tested in the simulation as shown in figure.6. Peak signal to noise ratio (PSNR) and normalized correlation coefficient (NCC) are compared to reflect the imperceptibility and robustness.

The PSNR comparison is shown in Table 1. It can be seen that the AES has the best performance on PSNR, but the variation is big for different images. This comes from the different energy distribution of the Y, Cb, Cr components in

TABLE 2. Extracted watermark with attacks.

Attack	Extracted Watermark				
	AES	MES	RCAES	CCAES	CCMES
Gaussian Noise (mean=0.4,var=0.01)					
Salt and pepper noise (density=0.1)					
JPEG Compression (Q=30)					
Cropping (1/4)					
Histogram equalization					
Median filter (3 × 3)					
Rotation (20°)					


























TABLE 3. NCC comparison with attacks.

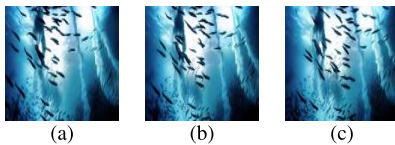
Attack	NCC				
	AES	MES	RCAES	CCAES	CCMES
Gaussian Noise (mean=0.4,var=0.01)	0.9387	0.9001	0.9640	0.9993	0.9998
Salt and pepper noise (density=0.1)	0.9717	0.8891	0.9912	0.9998	0.9998
JPEG Compression (Q=30)	0.9231	0.9682	0.9973	0.9686	0.9998
Cropping (1/4)	1	0.9877	1	0.9998	0.9998
Histogram equalization	0.9845	0.9925	0.9973	0.9998	0.9998
Median filter (3 × 3)	0.9720	0.9829	0.9773	0.9998	0.9998
Rotation (20°)	0.9307	0.9516	0.9709	0.9998	0.9998

TABLE 4. NCC comparison with SV exchange attack.

Cover Image	Attack Image	NCC				
		AES	MES	RCAES	CCAES	CCMES
Barbara	Boats	0.9425	0.9804	0.9980	0.9989	0.9998
	Lenna	0.8952	0.8855	0.9854	0.9857	0.9998
	Soccer	0.8532	0.8719	0.9861	0.9785	0.9998
	Baboon	0.7501	0.8041	0.9947	0.9976	0.9998
	Cable car	0.9742	0.9883	0.9965	0.9974	0.9998

TABLE 5. Extracted watermark with SV exchange attack.

Cover Image	Attack Image	Extracted Watermark				
		AES	MES	RCAES	CCAES	CCMES
Barbara	Boats					
	Lenna					
	Soccer					
	Baboon					
	Cable car					

**FIGURE 8.** Selected Host images. (a) Host image H_1 . (b) Host image H_2 . (c) Host image H_3 .








different images. The AES algorithm and MES algorithm use the Cb component to embed watermark, therefore the PSNR is closely related with the Cb component. While RCAES and CCAES have more stable PSNR for different kinds of images since more than one components are involved in the watermark embedding. The RCAES and CCAES has similar PSNR. The reason is that the Cb and Cr components are selected to insert watermark in the RCAES, which means that the effect of insertion in Y channel is least since Y channel has maximum energy. The PSNR of RCAES and CCAES is near to MES (such as Baboon, Pens and Soccer) or even overcomes MES (such as Pepper, Girl and Monarch) for some types of images. The CCMES has worst PSNR compared to the other schemes. The cover images Pepper with different schemes are shown in figure.7. It can be seen that the watermarked images with AES, RCAES and CCAES have good transparency, while MES and CCMES reduce the image quality.

We use Barbara as host image in the next tests. We compare the robustness against different kinds of attacks in Table 2 and Table 3. Extracted watermark and NCC are shown. It can be seen that the proposed RCAES, CCAES and CCMES have better performance than AES and MES

TABLE 6. PSNR of host images.






	Host image H_1	Host image H_2	Host image H_3
PSNR(dB)	55.3949	55.0849	54.1046

TABLE 7. NCC and extracted watermark with attacks in Video.

	NCC	Extracted Watermark
Gaussian Noise (mean=0.4,var=0.01)	0.9998	
Salt and pepper noise(density=0.1)	0.9998	
JPEG Compression(Q=30)	0.9943	
Cropping (1/4)	0.9998	
Histogram equalization	0.9998	
Median filter(3 × 3)	0.9976	
Rotation (20°)	0.9998	

for all kinds of attacks. CCMES is most stable and can achieve exact watermark recovery with NCC as 0.9998 for all attacks. CCAES has suboptimal results and also can achieve exact watermark recovery for most attacks only except for

TABLE 8. NCC and extracted watermark with SV attack in Video.

	Attack Image				
	Boats	Lenna	Soccer	Baboon	Cable car
NCC	0.9998	0.9998	0.9340	0.9993	0.9998
Extracted Watermark					

JPEG compression. For convolutional coding based schemes, the upper limit of NCC is 0.9998 because of the tail bit loss of the convolutional code. The performance of RCAES is little worse than CCAES because of two reasons: firstly, the code rate of RCAES is higher than CCAES. Secondly, convolutional code has stronger error correction ability than repetition code.

SV attack means the singular value exchange of the watermarked image and the attacking image. The AES is sensitive to SV attack. We investigate the effect of SV attack in the next. The extracted watermarks and NCC with SV exchange attack are shown in Table 4 and Table 5. It can be seen that CCMES has the best robustness for SV attack and can achieve exact recovery. The performance of CCAES is suboptimal and NCC is also bigger than 0.985.

From the above results, it can be seen that the CCMES has almost perfect robustness for all attacks, but the imperceptibility is worst. It is not feasible for real applications. Considering the two aspects of robustness and transparency, CCAES is the best choice, which can recover watermark quite well against all attacks without effect to the vision of host image.

B. SIMULATIONS FOR VIDEO

We choose the integrated optimal scheme CCAES and extend it for video watermarking. The test video “ocean” is downloaded from the internet with a length of about 45 seconds. After converting this video to frames, there are 1115 pieces of images. With the predefined keyframe H_1 , the most two similar frames H_2 and H_3 that found are shown as figure.8.

The PSNR of host images with watermark insertion is shown in Table 6. It can be seen that the three host images have similar PSNR, which is as high as about 54dB. The watermarking scheme can achieve better PSNR performance in video since the watermark information is spread into 3 host frames during the embedding process. The robustness performance against attacks is shown in Table 7 and Table 8. The CCAES can recover watermark quite well against all kinds of attacks for video.

VI. CONCLUSION

In this paper, we propose the robust non-blind watermarking schemes in YCbCr color space based on channel coding. It is shown that the channel based scheme can achieve exact watermark recovery against all kinds of attacks. Considering both robustness and transparency, the proposed CCAES is optimal. It can also achieve good performance for video

watermarking after extension. In the next, we will try to further optimize the scheme for video watermarking and implement blind extraction of the watermark.

REFERENCES

- [1] F. Hartung and M. Kutter, “Multimedia watermarking techniques,” *Proc. IEEE*, vol. 87, no. 7, pp. 1079–1107, Jul. 1999.
- [2] R. Koju and S. R. Joshi, “Comparative analysis of color image watermarking technique in RGB, YUV, and YCbCr color channels,” *Nepal J. Sci. Technol.*, vol. 15, no. 2, pp. 133–140, Feb. 2015.
- [3] S.-L. Hsieh, J.-J. Jian, I.-J. Tsai, and B.-Y. Huang, “A color image watermarking scheme based on secret sharing and wavelet transform,” in *Proc. IEEE Int. Conf. Syst.*, Montreal, QC, Canada, Jan. 2007, vol. 36, no. 7, pp. 2143–2148.
- [4] S. Maboul, E. Hassan, I. Elhaj, and D. Aboutajdine, “Robust color image watermarking based on singular value decomposition and dual tree complex wavelet transform,” in *Proc. IEEE Int. Conf. Electron.*, Marrakech, Morocco, Jan. 2008, pp. 534–537.
- [5] S. Rawat and B. Raman, “A new robust watermarking scheme for color images,” in *Proc. IEEE 2nd Int. Adv. Comput. Conf.*, Patiala, India, Mar. 2010, pp. 206–209.
- [6] M. Khalili, “DCT-Arnold chaotic based watermarking using JPEG-YCbCr,” *Optik-Int. J. Light Electron Opt.*, vol. 126, no. 23, pp. 4367–4371, Dec. 2015.
- [7] M. Moosazadeh and A. Andalib, “A new robust color digital image watermarking algorithm in DCT domain using genetic algorithm and coefficients exchange approach,” in *Proc. 2nd Int. Conf. Web Res.*, Tehran, Iran, Apr. 2016, pp. 19–24.
- [8] Y. Li, Y. Hao, and C. Wang, “A research on the robust digital watermark of color radar images,” in *Proc. IEEE Int. Conf. Inf. Automat.*, Harbin, China, Jun. 2010, pp. 1091–1096.
- [9] A. Al-Gindy, H. Al-Ahmad, R. Qahwaji, and A. Tawfik, “Watermarking of colour images in the DCT domain using Y channel,” in *Proc. IEEE/ACS Int. Conf. Comput. Syst. Appl.*, Rabat, Morocco, May 2009, pp. 1025–1028.
- [10] J. Advith, K. R. Varun, and K. Manikantan, “Novel digital image watermarking using DWT-DFT-SVD in YCbCr color space,” in *Proc. Int. Conf. Emerg. Trends Eng.*, Pudukkottai, India, Feb. 2016, pp. 1–6.
- [11] A. Roy, A. K. Maiti, and K. Ghosh, “An HVS inspired robust non-blind watermarking scheme in YCbCr color space,” *Int. J. Image Graph.*, vol. 18, no. 3, Jul. 2018, Art. no. 1850015.
- [12] L. Y. Xiang, Y. Li, W. Hao, P. Yang, and X. B. Shen, “Reversible natural language watermarking using synonym substitution and arithmetic coding,” *Comput. Mater. Continua*, vol. 55, no. 3, pp. 541–559, 2018.
- [13] D. Gong, Y. Chen, H. Lu, Z. Li, and Y. Han, “Self-embedding image watermarking based on combined decision using pre-offset and post-offset blocks,” *Comput. Mater. Continua*, vol. 57, no. 2, pp. 243–260, 2018.
- [14] Y. Wang, R. Ni, Y. Zhao, and M. Xian, “Watermark embedding for direct binary searched halftone images by adopting visual cryptography,” *Comput. Mater. Continua*, vol. 55, no. 2, pp. 255–265, 2018.
- [15] C. E. Shannon, “A mathematical theory of communication,” *Bell Syst. Tech. J.*, vol. 27, pp. 379–423 and 623–656, Jul. 1948.
- [16] D. J. Costello and G. D. Forney, “Channel coding: The road to channel capacity,” *Proc. IEEE*, vol. 95, no. 6, pp. 1150–1177, Jun. 2007.
- [17] S. Pereira, S. Voloshynovskiy, and T. Pun, “Effective channel coding for DCT watermarks,” in *Proc. Int. Conf. Image Process.*, Vancouver, BC, Canada, vol. 3, Sep. 2000, pp. 671–673.
- [18] R. Bao, T. Zhang, F. Tan, and Y. E. Wang, “Semi-fragile watermarking algorithm of color image based on slant transform and channel coding,” in *Proc. 4th Int. Congr. Image Signal Process.*, Shanghai, China, Oct. 2011, pp. 1039–1043.

- [19] S. Sarreshtedari and M. A. Akhaee, "A source-channel coding approach to digital image protection and self-recovery," *IEEE Trans. Image Process.*, vol. 24, no. 7, pp. 2266–2277, Jul. 2015.
- [20] W. A. Felcia and X. M. Binisha, "Protection and self recovery using dual watermark and source channel coding approach," *Int. J. Adv. Res. Electron. Commun. Eng.*, vol. 5, no. 3, pp. 617–620, Mar. 2016.
- [21] S. Sarreshtedari, M. A. Akhaee, and A. Abbasfar, "Source-channel coding-based watermarking for self-embedding of JPEG images," *Signal Process. Image Commun.*, vol. 62, pp. 106–116, Mar. 2018.
- [22] D. H. Hubel, *Eye, Brain, and Vision*. New York, NY, USA: Scientific American Library, 1988.
- [23] S. Lin, D. J. Costello, and M. J. Miller, "Automatic-repeat-request error-control schemes," *IEEE. Commun. Mag.*, vol. 22, no. 12, pp. 5–17, Dec. 1984.
- [24] S. Lin and D. J. Costello, Jr., *Error Control Coding: Fundamentals and Applications*. vol. 25, no. 1. Upper Saddle River, NJ, USA: Prentice-Hall, 1982, pp. 4–12.
- [25] G. Doerr and J. L. Dugelay, "A guide tour of video watermarking," *Signal Process., Image Commun.*, vol. 18, no. 4, pp. 263–282, Apr. 2003.
- [26] J. Li, Y. Wang, and S. Dong, "Video watermarking algorithm based DC coefficient," in *Proc. 2nd Int. Conf. Image, Vis. Comput. (ICIVC)*, Chengdu, China, Jun. 2017, pp. 454–458.
- [27] A. Cedillo-Hernandez, M. Cedillo-Hernandez, M. Nakano-Miyatake, and H. Perez-Meana, "A spatiotemporal saliency-modulated JND profile applied to video watermarking," *J. Vis. Commun. Image Represent.*, vol. 52, pp. 106–117, Feb. 2018.
- [28] M. Shanmugam and A. Chokkalingam, "Performance analysis of 2 level DWT-SVD based non blind and blind video watermarking using range conversion method," *Microsyst. Technol.*, vol. 24, no. 12, pp. 4757–4765, Dec. 2018.
- [29] H. Li, J. Qin, X. Xiang, L. Pan, W. Ma, and N. N. Xiong, "An efficient image matching algorithm based on adaptive threshold and RANSAC," *IEEE ACCESS*, vol. 6, pp. 66963–66971, 2018.
- [30] B. Xie, J. Qin, X. Xiang, H. Li, and L. Pan, "An image retrieval algorithm based on gist and SIFT features," *Int. J. Netw. Secur.*, vol. 20, no. 4, pp. 609–616, 2018.



YUN TAN received the M.S. and Ph.D. degrees from the Beijing University of Posts and Telecommunications, China, in 2004 and 2016, respectively. She is currently a Lecturer with the College of Computer Science and Information Technology, Central South University of Forestry and Technology. Her research interests mainly include information security, compressive sensing, and the Internet of Things.



JIAOHUA QIN received the B.S. degree in mathematics from the Hunan University of Science and Technology, China, in 1996, the M.S. degree in computer science and technology from the National University of Defense Technology, China, in 2001, and the Ph.D. degree in computing science from Hunan University, China, in 2009. She is currently a Professor with the College of Computer Science and Information Technology, Central South University of Forestry and Technology, China. Her research interests include network and information security, image processing, and pattern recognition.



XUYU XIANG received the B.S. degree in mathematics from Hunan Normal University, China, in 1996, the M.S. degree in computer science and technology from the National University of Defense Technology, China, in 2003, and the Ph.D. degree in computing science from Hunan University, China, in 2010. He is currently a Professor with the Central South University of Forestry and Technology, China. His research interests include network and information security, image processing, and the Internet of Things.



WENTAO MA received the B.S. degree in electronic science and technology from the Mingde College, Northwestern Polytechnical University, China, in 2017. He is currently pursuing the M.S. degree in information and communication engineering with the College of Computer Science and Information Technology, Central South University of Forestry and Technology, China. His research interests include pattern recognition and image processing.



WENYAN PAN received the B.S. degree in electronic and information engineering from Hunan City University, China, in 2017. He is currently pursuing the M.S. degree in computer technology with the College of Computer Science and Information Technology, Central South University of Forestry and Technology, China. His research interests include machine learning and image processing.



NEAL N. XIONG received the Ph.D. degrees from Wuhan University (about sensor system engineering), and the Japan Advanced Institute of Science and Technology (about dependable sensor networks), respectively. He is currently an Associate Professor (3rd year) with the Department of Mathematics and Computer Science, Northeastern State University, Tahlequah, OK, USA. Before he attended Northeastern State University, he worked in Georgia State University, Wentworth Technology Institution, and Colorado Technical University (full professor about 5 years) about 10 years. His research interests include cloud computing, security and dependability, parallel and distributed computing, networks, and optimization theory.

• • •